Grain refinement in as-cast 7475 aluminum alloy under hot deformation

R. Kaibyshev [a], O. Sitdikov [a,b], A. Goloborodko [a,b], T. Sakai [b,*]

[a] *Institute for Metals Superplasticity Problems, Khalturina 39, Ufa 450001, Russia*
[b] *Department of Mechanical Engineering and Intelligent Systems, The University of Electro-Communications, Chofu, Tokyo 182-8585, Japan*

Abstract

Grain refinement in an as-cast 0.16%Zr modified 7475 aluminum alloy was studied by means of compression at 490 °C and metallographic observations. The σ versus ε behavior shows a significant strain softening just after yielding and an apparent steady-state flow at strains of above 0.3. The structural changes are mainly characterized by development of deformation bands at an early stage of deformation ($\varepsilon \leq 0.3$), followed by new grain evolution during steady-state flow due to operation of grain boundary sliding (GBS). GBS can result in local lattice rotation and formation of deformation bands in the as-cast coarse grain interiors. The number and the misorientation angle of deformation bands increase with deformation, followed by evolution of new grains in high strain. It is concluded that grain refinement occurs by a deformation-induced continuous reaction; that is continuous dynamic recrystallization (CDRX). A key role of GBS and second phase dispersoids on CDRX is discussed in detail.

Keywords: Hot deformation; Aluminum alloy; As-cast structure; Grain refinement; Grain boundary sliding; Deformation band

1. Introduction

Grain refinement of aluminum alloys through hot working is of great practical importance because of enhanced mechanical properties of the products. It is known [1,2] that new grains are dynamically evolved even in aluminum alloys with high stacking fault energy (SFE) during hot deformation. As high SFE can promote the annihilation and rearrangement of lattice dislocations, conventional (i.e. discontinuous) dynamic recrystallization (DDRX), consisting of nucleation and long-distance growth of new grains, does not take place in commercial base aluminum alloys except highly pure aluminum [3–5]. Geometric dynamic recrystallization (GDRX) resulting from the impingement of serrated grain boundaries occurs in extremely elongated grains of severely hot-deformed aluminum and Al–5%Mg alloy [6–8]. Another and most likely mechanism of grain refinement can be continuous dynamic recrystallization (CDRX), which takes place under various thermomechanical processings (TMPs) of aluminum alloys [2,9–17]. CDRX generally involves the following processes; i.e. the formation of arrays of low angle boundaries and a gradual increase in the boundary misorientations during deformation, finally leading to new grain development in high strain [2]. CDRX was often observed during hot deformation of aluminum alloys with moderate density dislocation substructures, which are resulted from static recovery in heavily prior-deformed matrices [17] or evolved by previous TMPs [9–16]. There are, however, only few experimental data on grain refinement of as-cast and/or coarse-grained aluminum alloys [1,2].

The present study is aimed to examine the grain refinement taking place during hot working of an as-cast 0.16%Zr modified 7475 Al alloy. The alloy had a columnar coarse-grained structure and no well-defined subgrain structure. A specific attention is paid to elucidate main factors controlling grain refinement in the aluminum alloy and to discuss the mechanisms operated in detail.

* Corresponding author. Tel.: +81-42-443-5404; fax: +81-42-484-3327
E-mail address: sakai@mce.uec.ac.jp (T. Sakai).

2. Experimental procedure

A 7475 Al alloy was manufactured at the Kaiser Center for Technology by direct chill casting and had a chemical composition of Al–6%Zn–2.5%Mg–1.8%Cu–0.23%Cr–0.16%Zr–0.04%Fe–0.03%Si–0.03%Mn (in mass pct). The ingot was homogenized at 490°C for 20h. The initial microstructure is composed of dendrite lamellas lying parallel to the ingot axis, as it is shown in Fig. 1a. The boundaries of lamellar grains were rather straight and/or corrugated and the average size of the lamellas is in the range from 1 to 10 mm in the longitudinal direction and from 50 to 200 μm in the transverse one. Two types of dispersoids were identified as Al_3Cr and Al_3Zr by the TEM analysis of Fig. 1b. These particles are equiaxed, having average sizes of 100 nm (Al_3Cr) and 20 nm (Al_3Zr).

Cylindrical compression specimens with 10 mm in diameter and 12 mm in height were machined parallel to the ingot axis. Compression tests were carried out at constant crosshead speed using a Scheck RMS-100 testing machine at 490°C and at initial strain rates ranging from 10^{-5} to $10^{-2}s^{-1}$. A lubricant composed of oil and graphite was used to reduce friction. Strain-rate-jump test was also performed to determine the coefficient of strain rate sensitivity, m, as shown in Eq. (1):

$$m = \frac{\delta \ln \sigma}{\delta \ln \dot{\varepsilon}} \tag{1}$$

where σ is the true flow stress and $\dot{\varepsilon}$ is the true strain rate.

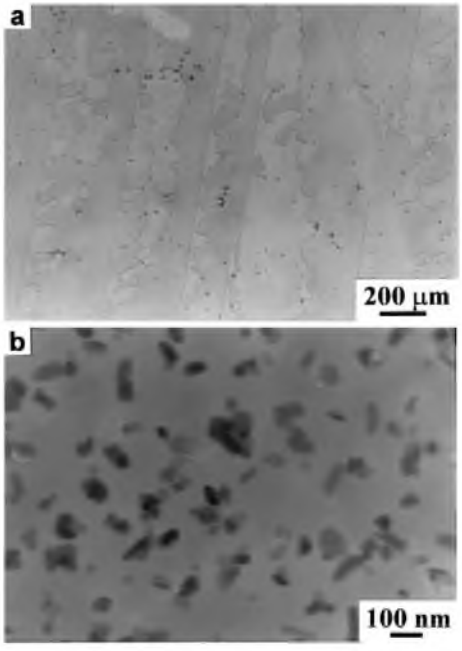

Fig. 1. Initial microstructure of 7475 Al alloy: (a) Optical and (b) TEM microstructures.

For microstructural examinations, the specimens were strained at an initial strain rate of $3 \times 10^{-4}\ s^{-1}$ to fixed strains of 0.16, 0.3, 0.7 and 1.4, immediately followed by quenching in water. Deformed microstructures were examined in the central region of a cross-section parallel to the compression axis after etching by a standard Dicks–Keller etchant. The metallographic analysis was carried out using a Neophot-32 microscope and an Epiquant automatic structure analyzer. Thin samples for transmission electron microscopy (TEM) were electropolished in a solution of 30% HNO_3 and 70% methanol at 25 V and at −30 °C. They were examined with a JEOL-2000FX TEM utilizing a double-tilt stage. (Sub)grain boundary misorientation distributions were obtained from electron back scattering diffraction pattern (EBSP) by using a Hitachi-3500A scanning electron microscope (SEM) with OIM™ software provided by TexSem Laboratories, Inc.

Surface examinations were carried out on some prior-polished samples deformed to $\varepsilon = 0.16$ at 490 °C. A sample deformed to $\varepsilon = 1.4$ was unloaded, repolished and additionally strained to $\varepsilon = 0.16$. For studying grain boundary sliding (GBS), some marker lines were scratched by diamond paste at an angle of 45° to the compression axis of the specimen, the surface of which was plated by aurum to prevent oxidation at high temperature. Surface observations were carried out using a JSM-840 SEM.

3. Experimental results

3.1. Mechanical behavior

A series of true stress–true strain (σ–ε) curves for the modified 7475 alloy at strain rates of 10^{-5}–$10^{-2}\ s^{-1}$ are depicted in Fig. 2a. At $\dot{\varepsilon} \leq 10^{-3}\ s^{-1}$, the flow curves show a sharp stress peak just after yielding and then significant strain softening followed by a steady-state flow at $\varepsilon \geq 0.3$. The flow softening in high strain appears less clearly as strain rate increases and almost disappears at $3 \times 10^{-2}\ s^{-1}$. The strain rate sensitivity, m, derived from the strain rate jump tests rises more clearly with decreasing strain rate even during the steady-state flow, as shown in Fig. 2b. This suggests that the steady-state flow in high strain can be apparent and resulted from continuous increment in true strain rate during constant crosshead speed compression. The σ–ε curves expected at constant strain rate test are shown by dashed lines in Fig. 2a. These will be discussed later in detail.

3.2. Structural changes during deformation

Typical optical microstructures developed during hot deformation are represented in Fig. 3. The boundaries of lamellar grains, roughly parallel to the ingot axis and

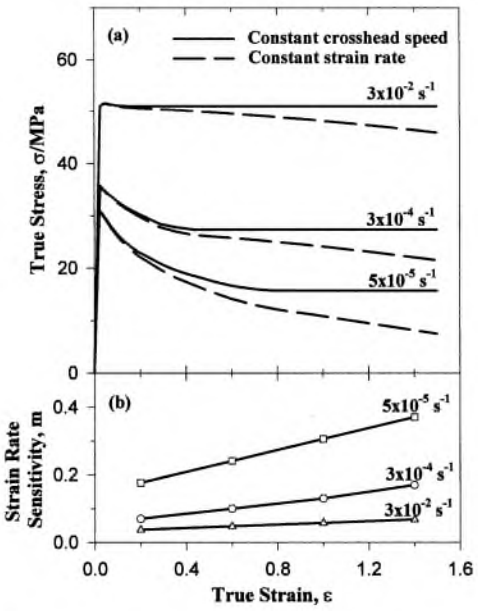

Fig. 2. (a) True stress–true strain curves of 7475 Al alloy tested at 490 °C and at various strain rates. The data were obtained from constant crosshead speed tests (solid line) and also evaluated from Eq. (5) for constant strain rates (dashed line). (b) Strain dependence of strain rate sensitivity, m.

so the compression direction, are gradually rotated by compression (Fig. 3a,b) and become almost perpendicular to the compression axis at $\varepsilon = 1.4$ (Fig. 3c). It can be clearly seen in Fig. 3b that the grain boundaries with coarse protrusions come in touch with each other, leading to evolution of new grains with an average size of around 20 μm, and that very fine grains are frequently developed along the original grain boundaries. It is also remarkable to see here that there are many deformation bands and subgrains developed in the original coarse grain interiors. With further straining to 1.4, the regions of new fine grains progressively increase in the coarse grain interiors and there is a mixed structure of remaining original grains and such developed new fine grains (Fig. 3c).

3.3. OIM microstructures

Typical orientation imaging microscopy (OIM) pictures of the 7475 alloy deformed to various strains are represented in Fig. 4. In these OIM maps, orientation differences (Θ) between neighboring grid points, $\Theta > 2^\circ$, $\Theta > 5^\circ$ and $\Theta > 15^\circ$ are marked by a thin gray, narrow and bold black lines, respectively. It can be seen in Fig. 4a that some new grains are evolved at along the corners of coarse protrusions and several boundaries with low to moderate misorientations are traversed and intersected in original grain interiors. The latters are considered to be similar to geometrically necessary dislocation boundaries (GNBs) or deformation bands [18]. This suggests that original coarse grains are

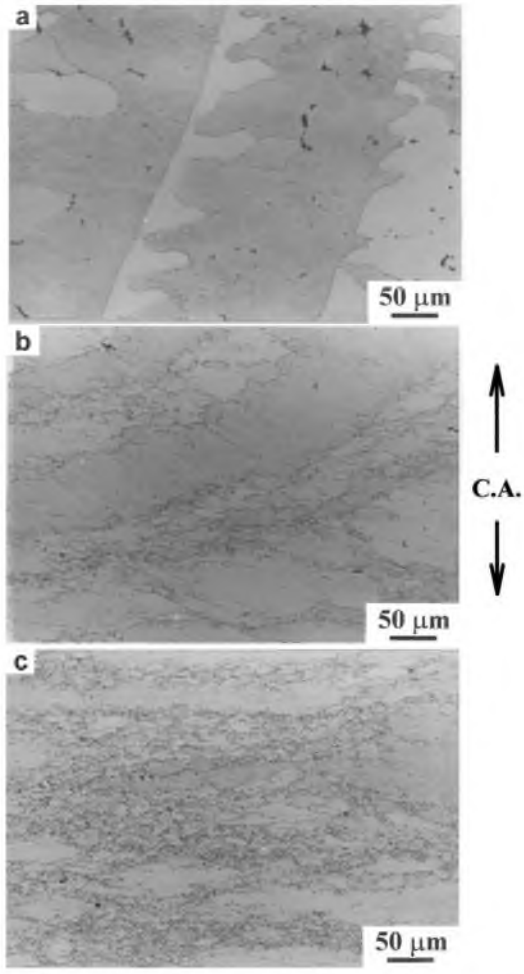

Fig. 3. Microstructural changes of 7475 Al alloy with deformation at 490 °C and at 3×10^{-4} s^{-1}. (a) $\varepsilon = 0.3$, (b) $\varepsilon = 0.7$ and (c) $\varepsilon = 1.4$. C.A. represents compression direction.

subdivided by those deformation bands even at early stages of hot deformation. Further deformation leads to increase in these misorientation angles and the numbers of GNBs. At a strain of $\varepsilon = 0.7$ (Fig. 4b), many fine grains with moderate to large angle boundaries are developed in colony accompanying with formation of relatively coarse grains with low to moderate angle boundaries. The latters may be transformed to the formers by further deformation.

Fig. 5 represents the point-to-point misorientation ($\Delta\Theta$) developed along the line T_1 in Fig. 4a and the line T_2 in Fig. 4b. Here the point-to-point misorientation defines a relative difference of crystal orientation between two adjacent scan points with a step of 1 μm. It is seen in Fig. 5a that $\Delta\Theta$ exceeds 4° at several local places, while it ranges from 1 to 2° in other ones. The formers and latters correspond to the GNBs evolved in coarse grain interiors and the boundaries of conventional subgrains developed, respectively. This suggests that local lattice rotation takes place along the initial grain boundaries, leading to inhomogeneous deforma-

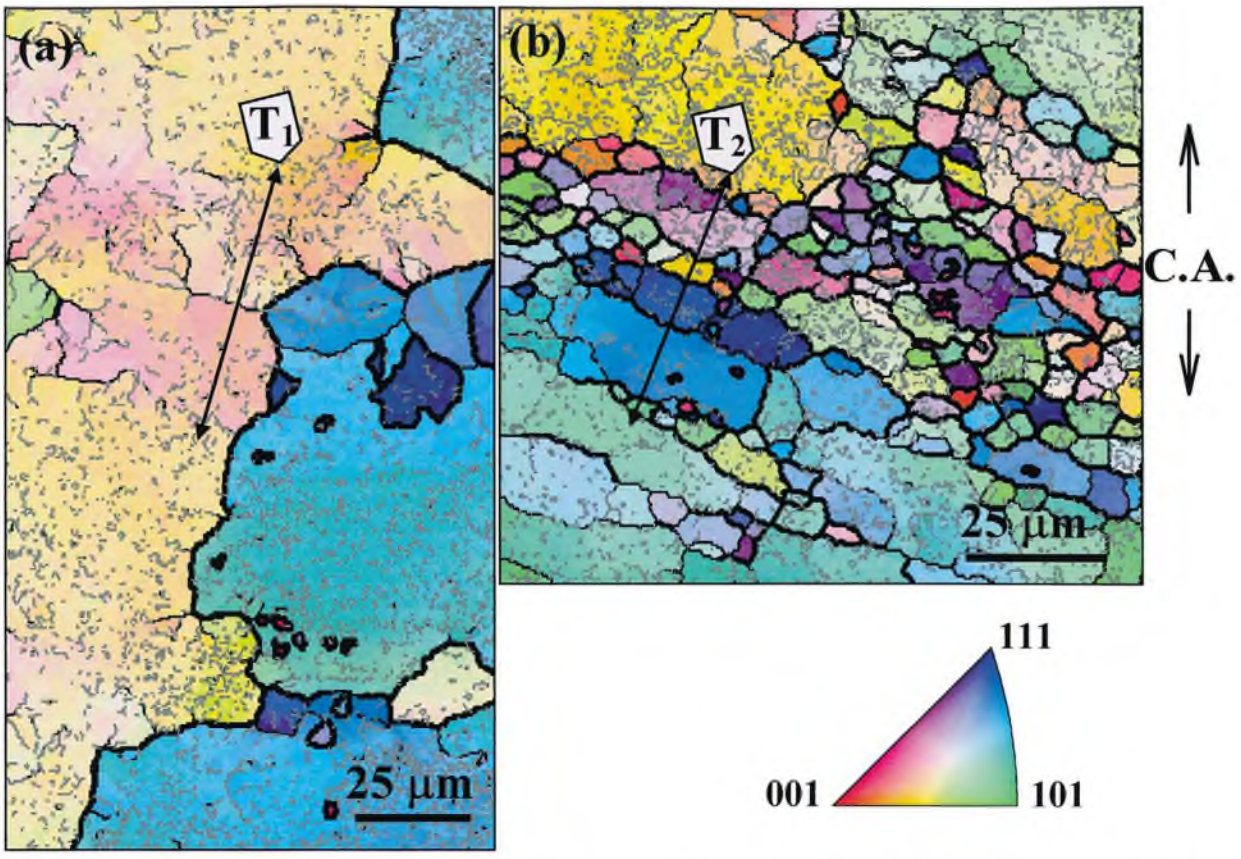

Fig. 4. OIM micrographs of 7475 Al alloy deformed to (a) $\varepsilon = 0.3$ and (b) $\varepsilon = 0.7$ at 490 °C and at 3×10^{-4} s^{-1}. Thin gray lines correspond to boundaries of misorientation $>2°$, thin black lines $>5°$ and bold line $>15°$, respectively.

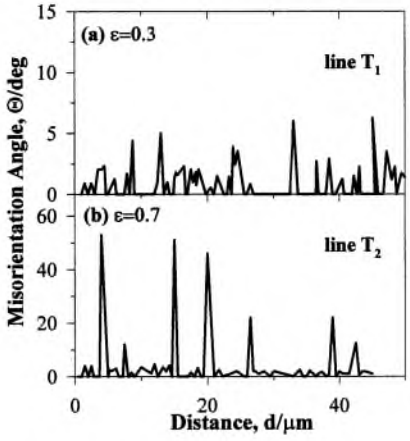

Fig. 5. Typical point-to-point misorientations ($\Delta\Theta$) developed in grain interiors of 7475 Al alloy deformed to (a) $\varepsilon = 0.3$ and (b) $\varepsilon = 0.7$ at 490 °C and at 3×10^{-4} s^{-1}. They were measured along the lines T_1 and T_2 indicated in Fig. 4a and b, respectively.

tion and then development of GNBs in coarse grain interiors even at $\varepsilon = 0.3$. With further straining to $\varepsilon = 0.7$ (Fig. 5b), high angle boundaries (HABs) with misorientations raging from 10° to beyond 50° are frequently developed in coarse grain interiors. This indicates that the numbers and the misorientations of GNBs developed at low strains rise rapidly with further deformation, leading to development of new fine grains. Fig. 6 shows OIM pictures of different places in the 7475 Al alloy deformed to a high strain of 1.4. The regions of new fine grains increase with further deformation, although the grain structure is highly inhomogeneous. It is interesting to note that crystal orientations of such new grains evolved in Fig. 6a are rather randomly distributed compared with those in Fig. 6b.

Fig. 7 shows changes in the misorientation distribution of low- and high-angle boundaries developed with deformation. At $\varepsilon = 0.3$, most of the boundaries have misorientations of below 5°. They transform into medium to high angle boundaries with deformation, leading to a rapid decrease in the fraction of low angle boundaries below 10°. Strain dependence of the average misorientation (Θ_{av}), the volume fraction (V_{rex}) and the average grain size (d) in the regions of newly developed grains are depicted in Fig. 8. Both Θ_{av} and V_{rex} start to increase at $\varepsilon \approx 0.2$ and rise with increasing strain, while d rapidly drops from around 20 μm at $\varepsilon = 0.3$ and approaches a constant value of about 6 μm at high strains above 0.6.

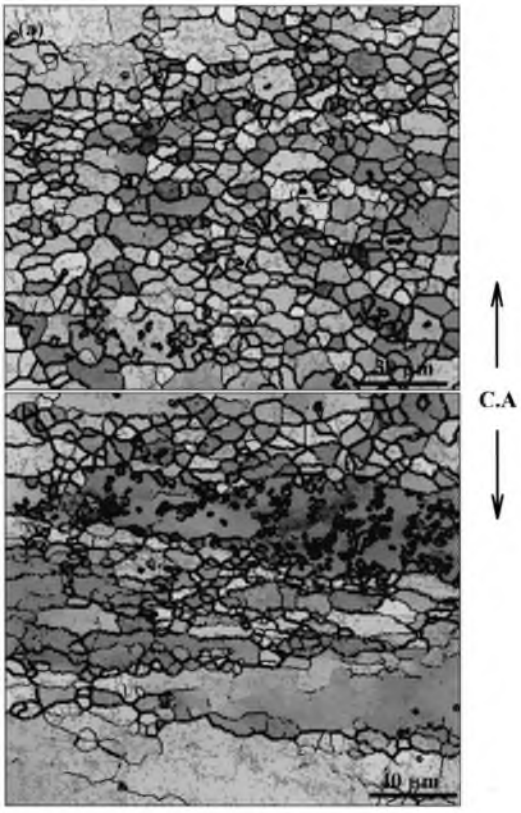

Fig. 6. Typical OIM micrographs in different places, (a) and (b), of 7475 Al alloy deformed to $\varepsilon = 1.4$ at 490 °C and at 3×10^{-4} s^{-1}. The lines have the same meanings as described in Fig. 4.

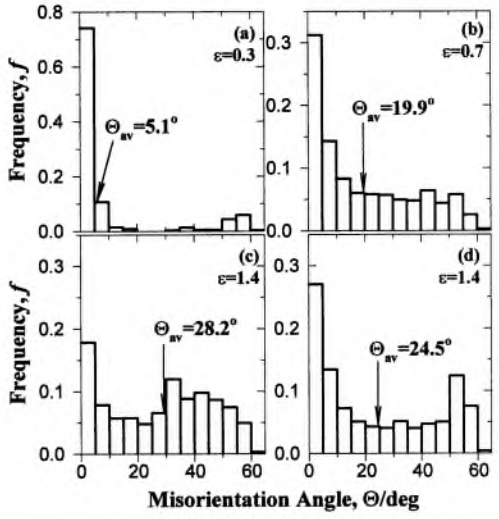

Fig. 7. Changes in misorientation distribution of dislocation boundaries and/or grain boundaries developed in 7475 Al alloy deformed at 490 °C and 3×10^{-4} s^{-1}. The data in (a), (b), (c) and (d) were obtained using Figs. 4a,b 6a,b, respectively.

4. Discussion

The present study showed that grain refinement takes place frequently in the as-cast modified 7475 aluminum alloy with coarse columnar grains during hot deformation. The features of this process can be characterized as follows.

i) Rapid flow softening takes place at an initial stage of hot deformation where new grains are not developed (i.e. $\varepsilon < 0.2$)
ii) Deformation bands are frequently developed in coarse grain interiors even in early hot deformation of the present aluminum alloy
iii) Grain refinement takes place near grain boundaries and then in grain interiors.

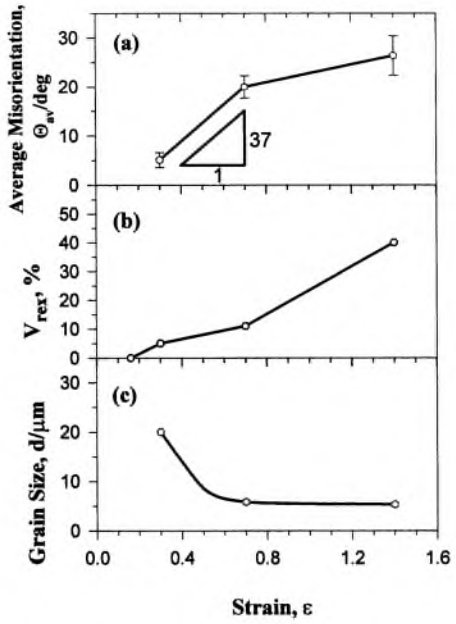

Fig. 8. Strain dependence of (a) the average misorientation of dislocation boundary and/or grain boundary, Θ_{av}, (b) the fraction of fine grain developed, V_{rex}, and the average grain size, d, in the regions of fine grains evolved. The 7475 Al alloy was deformed at 490 °C and at 3×10^{-4} s^{-1}.

4.1. Flow softening and new grain evolution

It is well known [19] that flow softening at high strains usually results from elimination of large number of dislocations by the long-distance migration of high angle boundaries under hot deformation. In the present case, however, significant flow softening takes place just after yielding where no new grains are formed. This indicates that the strain softening of the present alloy is caused by other mechanisms.[1] It is important to note in Figs .2b and 8 that m and V_{rex} start to increase at early stages of deformation and rise continuously with increasing strain. This suggests that the grain boundary sliding (GBS) takes place at present deformation conditions and plays an important role on fine-grained evolution and flow softening during deformation [20].

Surface morphology of the samples deformed to strains of 0.16 and 1.56 is shown in Fig. 9. It is clearly seen in Fig. 9 that GBS takes place even along the initial boundaries of coarse lamella grains and frequently in a fine-grained structure evolved at high strains accompanying with grain rotation. These are confirmed by slipping off and rotation of scratched marker lines as well as appearance of grain boundaries themselves. GBS should hardly operate in the initial layered structure since the boundaries are roughly parallel to the compression direction. These boundaries are, however, rotated and/or bended by small-strain deformation (Fig. 3a). Then GBS can occur along inclined parts of the original grain boundaries, which become roughly parallel to the maximum shear stress in compression. Under such conditions, GBS can easily take place and result in an early flow softening during deformation. With further straining to $\varepsilon > 0.3$, flow softening should take place more clearly due to new grain evolution at original grain boundaries and then in grain interiors, although the $\sigma - \varepsilon$ curves in Fig. 2 show a steady-state flow in high strain. Such a contradictory result is discussed as follows.

During compression at a constant crosshead speed, instantaneous true strain rate, $\dot{\varepsilon}$, increases with strain according to the following equation,

$$\dot{\varepsilon} = \dot{\varepsilon}_o \exp(-\varepsilon) \tag{2}$$

where $\dot{\varepsilon}_o$ is the initial strain rate. If flow stress can be approximated by a power-law function of strain rate [22],

$$\sigma = A\dot{\varepsilon}^m \tag{3}$$

then σ is expressed as,

$$\sigma = \sigma_o \exp(-m\varepsilon) \tag{4}$$

and so true stress (σ_o) at a constant true strain rate $\dot{\varepsilon}_o$ can be evaluated as,

$$\sigma_o = \sigma \exp(m\varepsilon) \tag{5}$$

Using the data of σ versus ε and m versus ε in Fig. 2 and Eq. (5), the σ_o–ε curves estimated at constant strain rate $\dot{\varepsilon}_o$ are presented by dashed lines in Fig. 2a. It is seen that no steady-state flow takes place in high strain at a constant strain rate. At low strain rates the values of σ_o rapidly drop in $\varepsilon < 0.2$ and then gradually decrease in high strain, because the volume fraction of new fine grains increases with deformation (Fig. 8b).

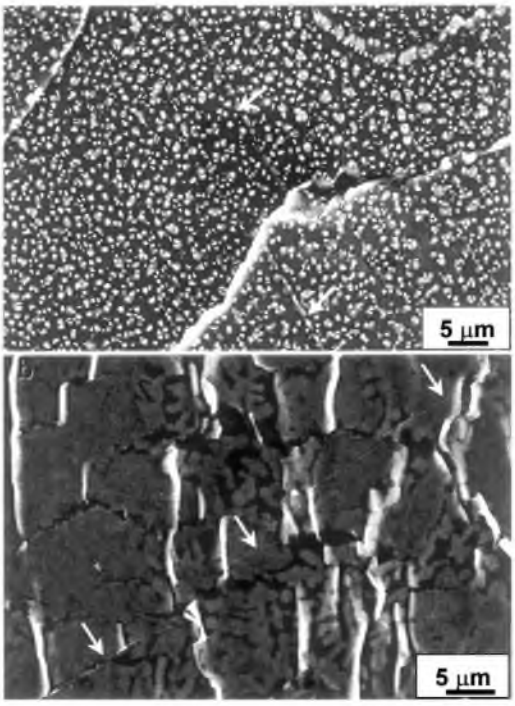

Fig. 9. Surface morphologies of 7475 Al alloy deformed at 490 °C and at 3×10^{-4} s^{-1}. (a) $\varepsilon = 0.16$ and (b) $\varepsilon = 1.56$. Arrows indicate the offsets of scratches along grain boundaries.

When hot deformation of fine-grained materials can be controlled mainly by GBS, the deformation equation is approximated by [22]

$$\dot{\varepsilon} = C_1 d^{-p} \sigma^n \exp(-Q/RT) \tag{6}$$

where C_1, $p > 0$, $n > 0$ are experimental constants, d is the grain size, Q is the activation energy for deformation and the others have usual meanings. When T, $\dot{\varepsilon}$, C_1 and Q are constant, σ can be expressed by

$$\sigma = C_2 d^{p/n} \tag{7}$$

where C_2 is a constant. When grain refinement gradually takes place during hot deformation, σ should decrease in accordance with Eq. (7), leading to flow softening. It is seen from Figs. 2 and 8 that the σ_o–ε relationship at 3×10^{-4} s^{-1} is qualitatively in agreement with the result of V_{rex}. It is concluded, therefore, that the flow softening in the present 7475 Al alloy is due to the operation of both GBS and the dynamic evolution of fine grains during hot deformation.

[1] The present 7475 Al alloy contains Mg and Cu atoms in solution as well as insoluble dispersoids (Fig. 1b). This suggests [20,21] that yield point drop resulting from dislocation dynamics can contribute to a work softening at an early stage of deformation ($\varepsilon < 0.05$). Indeed, such phenomena should appear, if the resistance of dislocation motion dragging a solute atmosphere is appreciable [20]. However, as it has been earlier shown for a 7075 Al alloy [20], the yield drop effect becomes negligibly small during high temperature deformation. It is evident from Fig. 2a that a very small amount of flow softening takes place just after yielding at a highest strain rate of 10^{-2} s^{-1}, when yield point phenomena is expected to be most prominent [20,21]. It means that the stress drop observed after small strains at strain rates of 10^{-3}–10^{-4} s^{-1} cannot be associated with dislocation motion dragging solute atmospheres.

4.2. Mechanisms of fine grain evolution

It is found from the present results described above that grain refinement is caused by the operation of various kinds of mechanisms. Fig. 3b suggests that the grain boundaries with coarse protrusions come in touch, leading to relatively coarse grains, and also very fine grains are frequently developed along the original grain boundaries. The former mechanism is considered as a kind of geometric dynamic recrystallization [6,7]; namely, the grain boundaries of protrusions begin to come into contact with each other during compression, causing the protrusions to pinch-off and to cut off from the grain matrix. This mechanism can operate in the strain interval 0.3–0.7 and provides the formation of relatively coarse grains. The average grain size of about 20 μm corresponds roughly to that of protrusions (Fig. 3b). Its contribution into the total process of grain refinement in the 7475 Al alloy, however, may be minor.

Another mechanism of grain refinement can be related to the development of significant strain gradients and then frequent evolution of deformation bands at relatively low strains. Figs. 3 and 4 show that many deformation bands and subgrains as well as very fine grains are developed rarely at $\varepsilon = 0.3$ and frequently at $\varepsilon = 0.7$ in coarse grain interiors. Let us discuss the development of deformation bands, grain subdivision and then a fine-grained structure during hot deformation. It was recently reported [23,24] that evolution of deformation bands following GNBs can play a key role in grain refinement during intense plastic deformation of some metallic materials at low to intermediate temperatures ($T < 0.5T_m$, where T_m is the melting point). Under such deformation conditions, GNBs, such as microband, kink or deformation band, etc. [18], are easily developed and the number and the average misorientation of these boundaries increase with increasing strain, finally leading to evolution of new fine grains [23,24]. In other words, the main mechanism of grain refinement can be directly associated with the grain splitting by a formation of internal GNBs followed by their transformation into large-angle boundaries. It has been clearly shown in [23] that such development of new fine grain structure is a consequence of a kind of deformation-induced continuous reactions, that is continuous dynamic recrystallization (CDRX).

The CDRX mechanism was found to operate in the as-cast coarse-grained Al alloy even under high-temperature deformation. It is known that, even if strain gradients are developed during hot deformation of conventional equiaxial-grained Al alloys, they could rapidly disappear due to frequent operation of dynamic recovery and GBS, and then such strain induced GNBs could be hardly developed [1–8]. The present as-cast aluminum alloy has, however, an unusual coarse lamellar grain structure with non-symmetric shapes, i.e. having alternating straight and corrugated grain boundary segments (Fig. 1a). When GBS takes place under such structural conditions, it may operate inhomogeneously and result consequently in development of inhomogeneous strain gradients followed by GNBs, as shown schematically in Fig. 10.

First the lamellar grain boundaries roughly parallel to the compression axis are rotated by early hot deformation, then GBS can start to operate on relatively straight boundary segments, but it still scarcely occurs on corrugated boundaries in the opposite side. As a result, highly inhomogeneous deformation can develop in the grain interiors and then provide formation of GNBs. Fig. 11 shows a typical deformation relief appearing in the surface of a specimen deformed to $\varepsilon = 0.16$. Some deformation bands as well as fine slip bands are developed even at such low strains. With further compression, the number of deformation bands increases and their mutual crossing leads to fragmentation of original grains into separate misoriented domains. Concurrently, the boundary misorientations of such domains grow rapidly with further deformation, finally followed by their transformation into high-angle boundaries. During such processes, GBS taking place frequently in new fine-grained regions can accelerate an increase in the boundary misorientation and assist a rapid development of fine grains with large angle misorientations [25].

Another factor promoting CDRX under hot deformation of the present Al alloy can be an effect of second phase particles, which provide a thermal stability of dislocation substructures [1,17,24] and prevent any relaxation of strain gradients. Fig. 12 shows typical TEM microstructures evolved in the present as-cast 7475 Al alloy at $\varepsilon = 0.3$ and 1.4. It is seen that there is some strong interaction between lattice dislocations and Al_3Zr/Al_3Cr nanoscale dispersoids. In addition, many precipitates are located along deformation-induced boundaries. This suggests that these dispersoids may restrict effectively an ability of lattice dislocation to long-range rearrangement and thus retard or prevent any relaxation of strain gradients developed in grain interiors. Strain gradients can be increased with further deformation, leading to development of GNBs there. This effect can additionally accelerate an increase in the misorientation of deformation-induced boundaries and their conversion into high-angle boundaries. It is concluded, therefore, that the stabilization effect of dislocation substructures due to second phase dispersoids should play an important role in operation of CDRX during hot deformation of the present Al alloy.

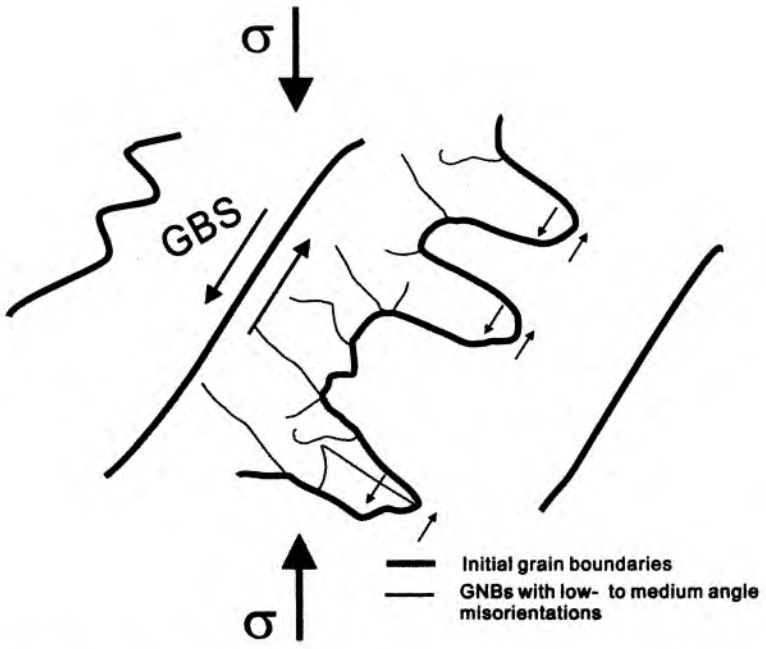

Fig. 10. Schematic representation for GBS taking place in corrugated lamellar grains with irregular shape, leading to development of inhomogeneous local strains and then GNBs.

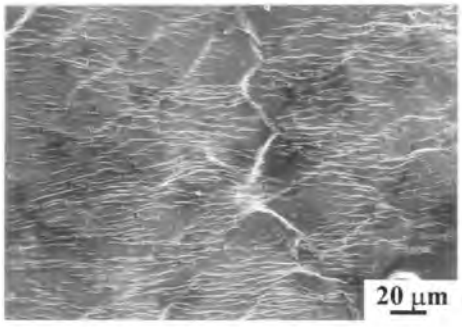

Fig. 11. Deformation relief for 7475 Al alloy deformed to a strain of 0.16 at 490 °C and at 3×10^{-4} s^{-1}.

5. Conclusions

Hot deformation of an as-cast 0.16%Zr modified 7475 aluminum alloy with a coarse-grained layered structure was studied by means of compression at 490 °C and metallographic observations. The main results are summarized as follows.

The deformation behavior at constant crosshead speed shows a significant strain softening just after yielding and an apparent steady-state flow at strains of above 0.3, although true stress estimated at constant strain rate test decreases monotonously with strain.

Grain boundary sliding (GBS) takes place first along rather straight and corrugated initial boundaries and frequently on the boundaries of new fine grains evolved during deformation. Flow softening taking place in high strain can result from both operation of GBS and dynamic evolution of fine grains.

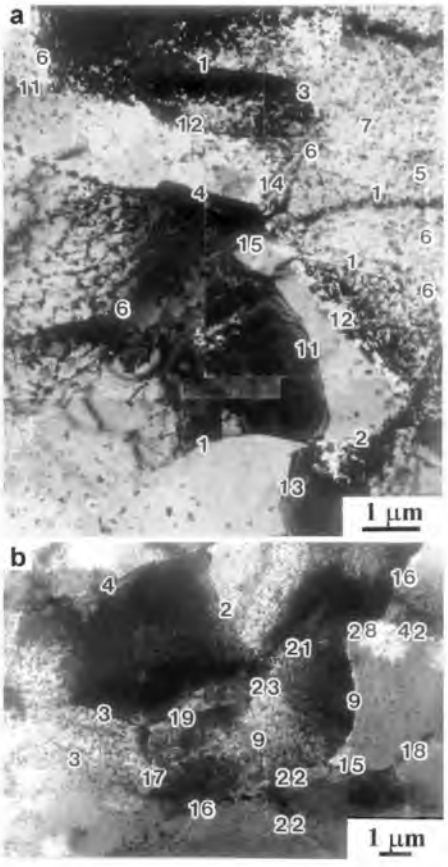

Fig. 12. Typical TEM structures of 7475 Al alloy deformed at 490 °C and at 3×10^{-4} s^{-1}, followed by water quenching. The numbers indicate dislocation boundary misorientation angles. (a) $\varepsilon = 0.3$ and (b) $\varepsilon = 1.4$.

GBS occurs inhomogeneously in the initial coarse and corrugated lamellar grains, resulting in local lattice rotation and formation of deformation bands at relatively low strains. Mutual crossing of deformation bands subdivides an original coarse grain into several misoriented domains.

The number and the misorientation angle of deformation bands increase with increase in strain, finally followed by their transformation into high-angle boundaries and evolution of new fine grains in high strain. This mechanism of grain refinement is similar to continuous dynamic recrystallization (CDRX).

Second phase dispersoids can serve as very effective stabilizers for dislocation substructures and deformation bands developed and, consequently, assist an increase in the misorientation of deformation–induced dislocation boundaries. This can also play a key role in initiation of CDRX.

Acknowledgements

O.S. would like to express his hearty thanks to the Japan Society for Promotion Science for providing a scientific fellowship. A.G. wishes to thank the Japanese Government for providing the scholarship.

References

[1] F.J. Humphreys, M. Hatherly, Recrystallization and Related Annealing Phenomena, Pergamon Press, Oxford, 1996, p. 497.
[2] S. Gourdet, F. Montheillet, Mater. Sci. Eng. A283 (2000) 274.
[3] H. Yamagata, Acta Metall. Mater. 43 (1992) 723.
[4] J.P. Lin, T.C. Lei, X.Y. An, Scripta Metall. Mater. 2 (1992) 1869.
[5] D. Ponge, M. Bredehoft, G. Gottstein, Scripta Mater. 37 (1997) 1769.
[6] M.R. Drury, F.J. Humphreys, Acta Metall. 34 (1986) 2259.
[7] J.K. Solberg, H.J. McQueen, N. Ryum, E. Nes, Philos. Mag. 60A (1989) 447.
[8] G.A. Henshall, M.E. Kassner, H.J. McQueen, Metall. Trans. 23A (1992) 881.
[9] B.M. Watts, M.J. Stowell, B.L. Baikie, D.G.E. Owen, Metals Sci. 10 (1976) 189.
[10] J.A. Wert, N.E. Paton, C.H. Hamilton, M.W. Mahoney, Metall. Trans. 12A (1981) 1267.
[11] S.J. Hales, T.R. McNelley, Acta Metall. 36 (1988) 1229.
[12] H. Gudmundsson, D. Brooks, J.A. Wert, Acta Metall. Mater. 39 (1991) 19.
[13] Q. Liu, H. Huang, M. Yao, J. Yang, Acta Metall. Mater. 40 (1992) 1753.
[14] J. Liu, D.J. Chakrabarti, Acta Mater. 44 (1996) 4647.
[15] X. Yang, H. Miura, T. Sakai, Mater. Trans. JIM 37 (1996) 1379.
[16] T. Sakai, H. Yang, H. Miura, Mater. Sci. Eng. A234–236 (1997) 857.
[17] T.G. Nieh, L.M. Hsiung, J. Wadsworth, R. Kaibyshev, Acta Mater. 46 (1998) 2789.
[18] B. Bay, N. Hansen, D.A. Hughes, D. Kuhlmann-Wilsdorf, Acta Metall. Mater. 40 (1992) 205.
[19] T. Sakai, J.J. Jonas, Acta Metall. 32 (1984) 189.
[20] T. Sakai, C. Takahashi, Mater.Trans. JIM 32 (1991) 375.
[21] T. Sakai, H. Miura, N. Muramatsu, Strength of Materials, Proc. 10th ICSMA, Sendai, JIM, pp. 795–798.
[22] T.G. Nieh, J. Wadsworth, O.D. Sherby, Superplasticity in Metals and Ceramics, Cambridge Univ. Press, Cambridge, 1997, p. 273.
[23] A. Belyakov, T. Sakai, H. Miura, K. Tsuzaki, Philos. Mag. A81 (2001) 2629.
[24] O. Sitdikov, R. Kaibyshev, I. Safarov, I. Mazurina, Phys. Metal. Metallogr. 92 (2001) 270.
[25] X. Yang, H. Miura, T. Sakai, Mater. Trans. 43(10) (2002) in press.